International Journal of Fracture 33: 297–312 (1987)

A review of indentation fracture theory: its development, principles and limitations

P. OSTOJIC and R. McPHERSON
Department of Materials Engineering, Monash University, Clayton, Australia

Received 14 April 1986; accepted in revised form 28 October 1986

Abstract

The influence of 'blunt' and 'sharp' indenters in producing indentation crack patterns is outlined. Attention is then focused on the initiation and propagation of cracks formed during a sharp contact event as such contacts are of the most practical interest and are commonly used to determine the fracture toughness of opaque materials. The modifying influence on the behaviour of such cracks as a result of anisotropy, particle size, environment and residual stress effects is briefly discussed. A simplistic derivation of the current formula used in determining the fracture toughness of suitable materials from a sharp contact event is then given. The criteria for valid results are also presented and these, in conjunction with other points discussed, highlight some of the limitations of this method of toughness testing.

1.0. Introduction

The literature on indentation fracture mechanics is extensive and results from the relevance of this field to practical applications. Indentation fracture theory has, for example, provided an insight into machining damage, erosion and wear phenomena and is gaining widespread acceptance as a simple and accurate means of determining the toughness of brittle materials. The abundance of literature can, however, be daunting to a newcomer in the field attempting to gain an understanding of the development, basic theory and limitations of indentation fracture mechanics. It is the purpose of this work then, to provide a review paper aimed at outlining these aspects of indentation fracture. The emphasis of this review is directed towards indentation toughness testing as this area has, perhaps, generated the most interest.

As sharp contact events are generally of the most practical interest, discussion will be centred about them, although much in regard to propagation of these type of indentation induced cracks is equally applicable to blunt contacts.

2.0. Types of indentation cracking

Indentation induced crack patterns generally result from contacts that may be classified as either 'blunt' or 'sharp' [1].

2.1. Blunt indenters

Contacts which are essentially *elastic* in nature up to the point of fracture may be regarded as 'blunt' as, for example, those usually produced by spherical indenters in brittle materials at low loads.

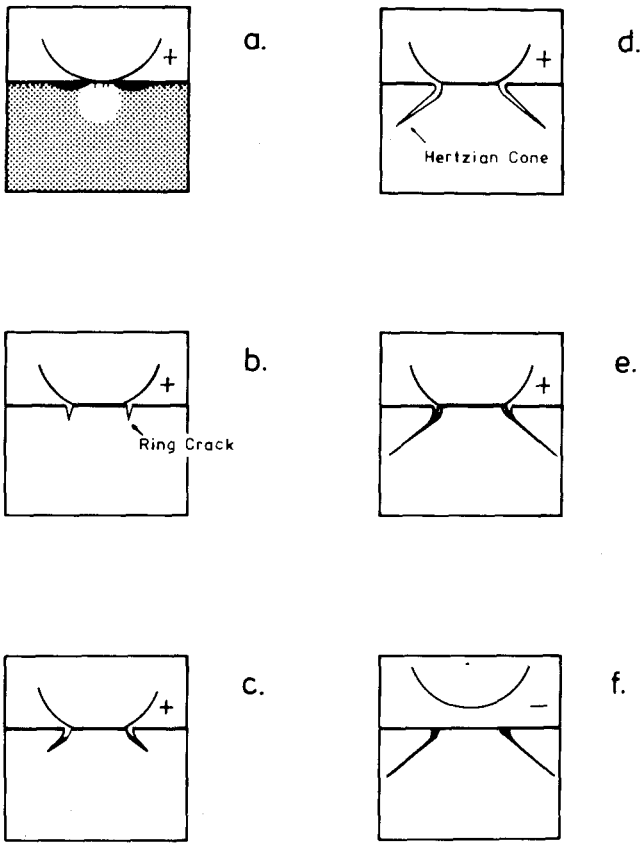

Fig. 1. Evolution of the Hertzian cone crack during blunt indenter loading (+) and unloading (−). The tensile (black) and compressive (unshaded) stress fields are shown in Fig. 1a (from Lawn and Marshall, [17]).

The first successful attempt at the analysis of such contacts was that of Hertz in 1882 [2]. Since then, these contacts have been extensively studied and characterised [3–8]. Phenomenologically, the contacts may be described as follows (Fig. 1):

As the spherical indenter contacts the surface the applied load is distributed over the contact site as compressive stresses. Elastic deformation of the material, both at and around the contact site, gives rise to tensile stresses confined to a shallow 'skin' outside this region and compressive stresses immediately below (Fig. 1a). As the contact zone size increases, so too does the magnitude of the tensile and compressive stresses. The tensile field moves out with the expanding zone until a suitable flaw is found i.e. a flaw whose orientation and size are such that it becomes unstable. When this occurs the flaw forms a surface 'ring' crack which, following the maximum tensile field, completely encircles the indenter while at the same time driving downwards into the material. This downward motion of the ring crack is, of course, arrested as the crack extends out of the surface tensile skin region (Fig. 1b).

Further loading results in expansion of the contact and stable downward growth of the ring crack which deviates outwards to avoid the compressive field below the indenter (Fig. 1c).

As loading continues, so too does the driving force until a condition is reached where the ring crack becomes unstable and spontaneously forms a fully developed Hertzian cone crack (Fig. 1d).

The crack continues to advance into the material in a stable manner as the load is increased until the contact site engulfs the surface ring crack. This results in crack closure and may also give rise to higher order (secondary, tertiary etc.) ring crack formation (Fig. 1e).

On unloading, the material attempts to minimise its stored elastic and surface energy by crack closure and healing. It is prevented in doing this however by the presence of debris wedged into the crack, environmental effects, fracture steps etc. In fact, it has been reported that a lateral displacement of as little as 1 in 1000 is sufficient to prevent total crack closure [9] and it is these effects which allow the crack to remain visible upon complete unloading (Fig. 1f).

2.2. Sharp indenters

In contrast to blunt indenters, a contact which is essentially *plastic* in nature up to the point of fracture is said to be 'sharp'. A well-known example of such a contact is that produced by a standard Vickers hardness testing machine.

A simplistic, descriptive account of sharp indenter crack formation - ignoring crack initiation (discussed later) - would begin with the indenter contacting and penetrating the

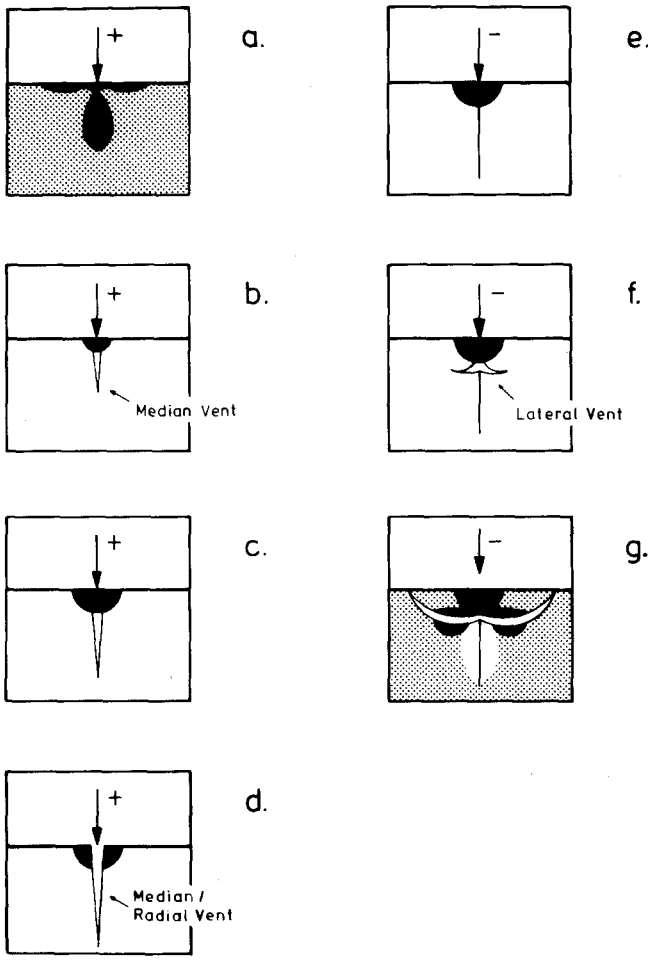

Fig. 2. Evaluation of the median, radial and lateral crack systems during sharp indenter loading (+) and unloading (−). The black region appearing in each figure indicates the plastic zone. Point loading and residual stress fields are shown in Figs. 2a and 2g respectively. The black and unshaded regions in these figures represent tensile and compressive stress fields respectively (after Lawn and Marshall, [17]).

specimen surface. This penetration leads to a plastically deformed zone surrounding the indentation site and gives rise to surface tensile zones adjacent to the contact, as well as a sub-surface tensile stress field immediately beneath the indenter tip (Fig. 2a). The penetration may also produce a totally contained, sub-surface, 'penny-like' crack (or 'vent') immediately under the point of the indenter where sub-surface tensile stresses are greatest (Fig. 2b). Further loading results in both downward and outward growth of this so-called 'median' crack (Fig. 2c) although outward growth is somewhat inhibited by near-surface compressive stresses. Median vent formation is further discussed in Section 3.2 (see also Fig. 8).

Further loading results in a situation where, for heavily loaded specimens, the sub-surface median penny-like cracks are able to break through these confining stress lobes and intersect the specimen surface forming half-penny surface 'median-radial' cracks (Fig. 2d). For a specimen not as heavily loaded, the median penny-like cracks remain sub-surface during the loading cycle, extending downwards and slightly outwards along principal normal stress contours (see Section 3.2) breaking through to the surface only during the unloading cycle when the intensity of the confining compressive stresses has been sufficiently reduced.

Upon unloading, the median vents attempt to close up but, once again, are prevented from doing so by debris and the existence of a residual stress field caused by the indented material attempting to accommodate the plastic deformation zone i.e. elastic-plastic mismatch (Fig. 2e). This residual stress field gives rise to saucer-shaped 'lateral' cracks which originate at the base of the plastic zone and extend in a plane parallel to the specimen surface as the specimen is unloaded (Fig. 2f). These lateral cracks continue their extension after indenter removal (Fig. 2g) under the influence of the residual stresses which may also drive partially developed sub-surface median cracks to completion, i.e. half-penny surface radials [10].

The lateral vents may intersect the surface resulting in the formation of chips which tend to obscure the indentation pattern. It has been found that the extent of lateral crack formation increases as load increases thereby indicating chipping to be more likely in a heavily loaded body [11].

2.3. Blunt-sharp indenters

Wiederhorn and Lawn [12] showed the effect of overloading a blunt indenter. Using soda-lime glass and a spherical indenter, they produced the expected Hertzian cone crack at loads of approximately 100 N. However increasing the load to 500 N resulted in the formation of median and lateral vents typical of sharp indenters, although these were somewhat inhibited by the pre-existing Hertzian cone crack. This result was later supported by impact damage studies on fused silica [13]. 'Sharp' indenters may also behave as 'blunt' indenters in that they may produce Hertzian cones prior to median-radial crack formation if the tip of the indenter is somehow blunted, i.e. if the tip is flattened on contact or if the material contains a large number of flaws (as might occur, for example, in a highly porous body [14]).

At high loads then, a spherical indenter is effectively able to 'penetrate' the specimen surface and behave much like a sharp indenter. Similarly, in some situations, sharp indenters are able to behave in much the same fashion as blunt indenters.

During their indentation studies on single and polycrystalline brittle materials, Evans and Wilshaw [15] chose the radius of curvature of their conical indenters such that a sharp crack pattern was produced. Their results showed that care must be taken in choosing a suitable radius of curvature to produce a sharp indent in a given material and that the same indenter might not produce a sharp indent in *all* materials. Their results supported the earlier work of Lawn and Fuller [10] who were able to produce cone fracture before median cracking by using a pyramidal indenter of 160 deg included angle.

Thus, in any indentation study care must be taken in choosing a suitable indenter and load so that the required crack pattern (blunt or sharp) is achieved.

Although both blunt and sharp indenter crack patterns may be used to determine material fracture toughness [4,16], sharp indenters are more suited to this purpose in opaque materials since they produce a surface crack which can be related to the material fracture toughness. Blunt indenters on the other hand, rely on the critical load necessary to spontaneously form a Hertzian cone crack from the precursory ring crack as the basis for determining fracture toughness. Since this is a sub-surface phenomenon, the formation of the Hertzian cone is not readily observable at the specimen surface in an opaque material and so is not as amenable to fracture toughness determination in these materials as sharp indenters. Further, crack formation with sharp indenters typically occurs at loads a few orders of magnitude less than for blunt indenters [17] allowing for the use of a smaller testing machine.

3.0. Principles of indentation-induced cracking: sharp indenters

The stress field about an indentation is usually described by three components; stresses radiating from the point of contact (radial stresses), stresses which encircle the contact (hoop stresses) and shear stresses. It is the behaviour of these stresses in the immediate vicinity of the contact (the so-called 'near-field' stresses) which determine the point of initiation of the indentation induced cracks. These stresses at points far removed from the contact (the 'far-field' stresses) also determine the path of propagation of the same cracks.

The interaction of these stresses in both the near and far fields gives rise to a maximum tensile stress. Since it is this stress which plays the major role in the initiation and propagation processes it will be discussed in some detail.

3.1. Initiation

Lawn and Evans [18] proposed a working model for predicting the onset of median cracking below a sharp indenter acting on a reasonably well finished, brittle body. In this model, the plastic zone is formed by the radial movement (by cracking, densification etc) of that volume of material displaced by the indenter. This gives rise to an elastic-plastic stress field analogous to that produced by an expanding spherical void subjected to an internal hydrostatic force distribution (the so-called 'expanding cavity' model of plasticity theory, [19–21]).

The Lawn-Evans model makes use of this analogy as well as the work of Lawn and Swain [22] who found the maximum tensile stress in a sharp contact event occurs directly below the indenter point at the elastic-plastic interface. Lawn and Evans argued that increasing the load increases the plastic zone size and hence, the position of the elastic-plastic boundary, leaving the tensile stress at the boundary constant. The maximum tensile field could then be viewed as effectively 'searching' the material below the contact for a suitable flaw. Once found, this flaw becomes unstable in the tensile field and ultimately forms the classic median vent.

The existence of fortuitous flaws in the vicinity of the contact site was inherently assumed in this early model. In a later indentation study involving deformation behaviour beneath sharp contact events in glasses of various composition, Hagan [23] showed that initiation of median and lateral cracks could also result from indentation-induced deformation beneath the contact site. For 'normal glasses' such as commercial soda-lime-silicate glass, plastic deformation resulted from sequential flow of the material as loading progressed. The resulting flow lines were found to be capable of initiating cracks and voids along their length or at their points of intersection [24].

Plastic flow in 'anomalous glasses' (e.g. fused silica) was not observed. Instead, compaction of the open silica structure occurred. Expansion of this compacted zone could lead to median cracking at the base of the zone during loading, while strain mismatch on unloading could give rise to lateral cracking [25].

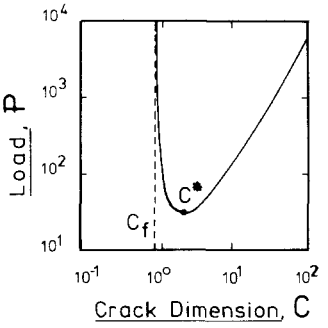

Fig. 3. The reduced crack dimension (C) as a function of the reduced load (P) at equilibrium according to the model proposed by Lawn and Evans, [18].

Using various materials (WC, SiC, Si etc.) Lawn and Evans were able to demonstrate the effect of loading on cracks of various sizes (Fig. 3). Small flaws below a critical size (C_f in Fig. 3) could not be made to extend whereas large flaws ($C > C^*$) grew stably with increasing load. Only flaws of a critical intermediate size ($C_f < C < C^*$) would become unstable and spontaneously form sub-surface median cracks at constant load. Lawn and Evans were able to derive equations for the maximum load and flaw size required to initiate a median flaw.

Lawn and Evans' initial work suggested then, that sub-surface median cracks formed first immediately below the indenter tip eventually giving rise to the surface median-radial cracks.

However, the expanding cavity model on which the Lawn-Evans proposal is based requires a uniform distribution of contact pressure across the face of the indenter. Investigations into the stress distribution across the face of various wedge-shaped diamond indenters acting on assorted materials (both metals and plastics) showed the condition for uniform stress distribution to be met only when the indenter angle was acute (< 90 deg) and the ratio of Young's modulus (E) to yield stress of the material was high. The results were also claimed to be applicable to pyramidal indenters [26].

Perrot [27], making use of these results, claimed that since Vickers indentations involve indenter angles of 136 deg, the stress distribution was not analogous to the expanding cavity model. Further, the Lawn-Evans model assumed no plasticity of the test material and so was limited to only extremely brittle materials. A further objection to the Lawn-Evans model was that the (calculated) flaw size required for median crack initiation in some materials (i.e. NaCl) was such that, according to this model, they should be readily detectable. However, no such flaws could be found [28].

Perrot [27] provided an analysis of the stress field about an axially symmetric, obtuse indenter in a body which exhibits some plasticity i.e. an indentation in which the volume of material displaced by the indenter is 'piled-up' about the impression. His results indicated that the maximum tensile field occurred at the corners of the indentation and was confined to a shallow surface region within the plastic zone. It was this field he claimed, which gave rise to the surface radial - or 'Palmqvist' (after Palmqvist [29]) - cracks observed by various workers before the onset of median cracking [15,30–32].

Lankford [33] proposed that the Lawn-Evans model was basically correct and erred only in its assumption of median initiation preceding radial. He suggested that this fault could be overcome in the case of Vickers indentations by adopting the Perrot model of a near-surface maximum tensile stress as opposed to the Lawn-Evans model of a sub-surface maximum tensile stress.

In this approach then, the highly tensile near-surface field, as described by Perrot, 'searches' the plastic zone for a suitable surface flaw from which to form a radial (Palmqvist) crack (Fig.

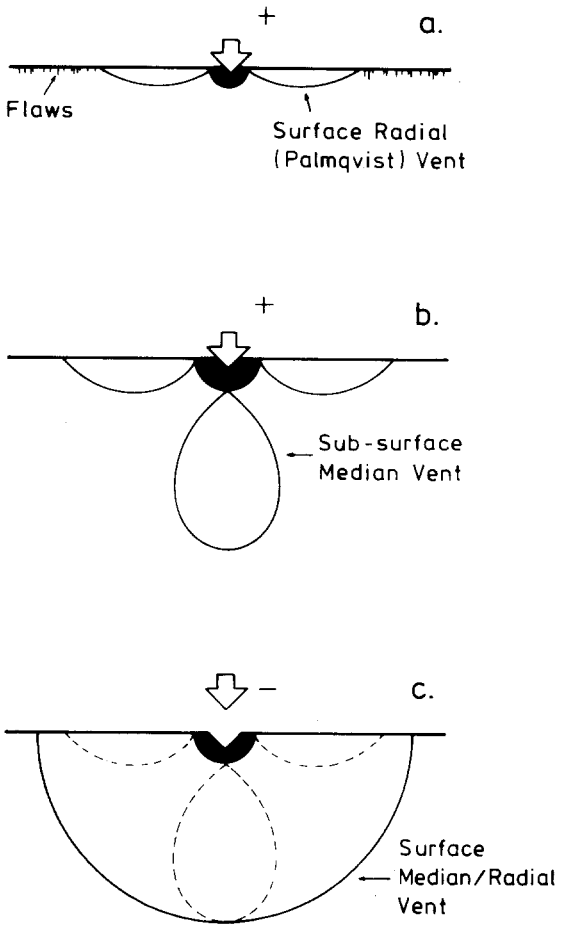

Fig. 4. The model proposed by Lankford [33] for fracture initiation beneath a sharp (Vickers) indenter. In this model, radial crack initiation (Fig. 4a) precedes median (Fig. 4b). Loading (+) and unloading (−) cycles are as shown.

4a). Surface finish would then be expected to influence the radial crack initiation load and this was, indeed, observed [15,34].

Further loading results in sub-surface penny-like crack formation (Fig. 4b). Upon unloading, these cracks were thought to merge with the surface radial cracks to form the classic median-radial crack pattern (Fig. 4c).

Chiang, Marshall and Evans [35], however, claimed the Lankford-Perrot model to be incorrect on a number of points including the position and nature of the surface stresses. The Perrot model requires the near-surface stresses to be tensile and confined to the plastic zone. However, radial cracks have been observed to *terminate* within the plastic zone indicating a compressive stress [15,36,37]. Further, radial cracks have been observed to extend outside the plastic zone [33] indicating the stress field to be more extensive than envisaged by Perrot.

Chiang et al. also claimed that materials subjected to large (included) angle indentations, or materials of low Young's modulus, deform by radial compression resulting in very little material pile-up about the impression site and a (usually) hemispherically symmetric plastic zone. The occurrence of this phenomenon, even in materials which exhibit considerable plasticity such as annealed brass, suggests the Lawn-Evans model to be less restrictive than indicated by Perrot.

They then provided their own analysis of the near-field stresses for both pyramidal and

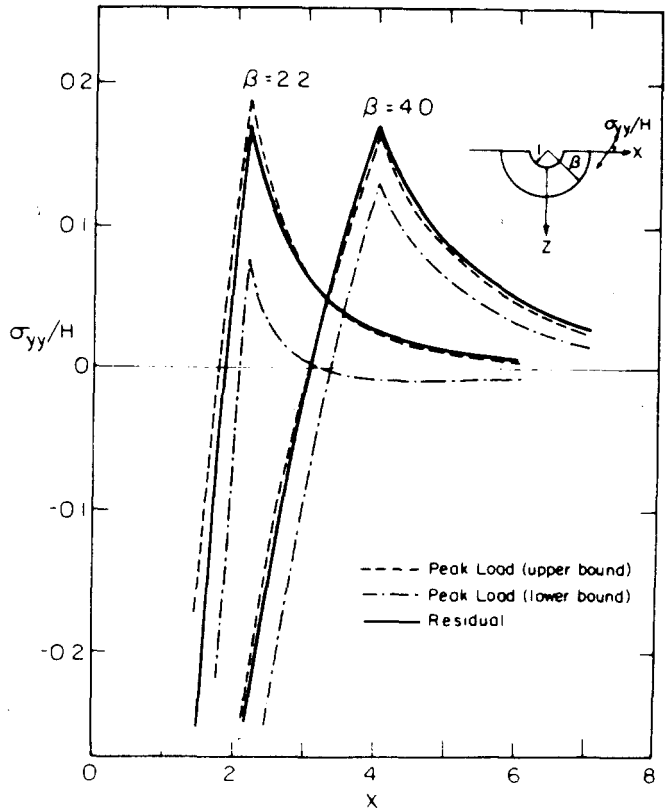

Fig. 5. Tangential surface stresses for radial fracture at both peak indenter load (upper and lower bounds) and indenter removal (residual), for two choices of relative plastic zone size (β). From Chiang, Marshall and Evans, [35].

spherical indenters taking into account the effect of the free surface (hemispherical cavity model) previously overlooked in both the Lawn-Evans and Perrot models. Their results showed that, regardless of the crack system:

(1) Maximum tension occurred at the elastic-plastic boundary,
(2) The maximum tension decreased rapidly within the plastic zone which is highly compressive and,
(3) The maximum tension decreased monotonically as it entered the elastic zone.

Their analysis also provided information specific to particular crack systems. For radial cracking, the residual tensile surface stress approximates or exceeds the peak load tensile surface stress depending on the material and the indenter size (Fig. 5). However, geometric factors involving the indenter angle indicate radial (and lateral) cracking should be suppressed during loading for large indenter angles i.e. Vickers indenters. This is consistent with observed behaviour [16].

For median cracks, the peak load tensile stress beneath the indenter always exceeds the residual stress but is less than the surface tensile stress.

Chiang et al. then applied the results of their analysis to the problem of crack initiation and found that radial cracks are, indeed, the first to initiate [38]. This results from a combination of the high surface tensile field and the availability of surface flaws. These cracks grow on unloading into both the plastic zone, where they are quickly terminated, and the elastic zone.

Larger loads are required as the surface finish improves so that a greater number of flaws may be 'sampled'. If the surface finish is very good or surface compressive stresses are introduced, radial crack formation may be suppressed and median cracks formed on unloading.

In situations where the surface flaw density is low and the material exhibits plasticity, sub-surface flaws may form from nuclei originating from intersecting shear or slip bands [24,28,39,40]. These nuclei grow under the influence of the near-field maximum tensile stress ultimately forming surface radial cracks on unloading.

This phenomenon also extends to many brittle (low E) materials which have now been found to exhibit micro-plasticity during indentation loading [41–44] and is thought to result in median crack nucleation in situations where the sub-surface flaw density is low [38]. Some evidence exists however, for the formation of median cracks from surface flaws in some glasses [34,43].

However, for the purposes of measuring fracture toughness from, for example, Vickers indentations a well-developed median crack is required. This necessitates a load in excess of that required to produce radial cracking although some work has been done in determining fracture toughness from Palmqvist cracks [45,46].

In these situations radial cracks are the first to nucleate, either from surface flaws or by plasticity, at a very early stage in the loading cycle. They are prevented from developing, however, until the unloading cycle. As the loading cycle continues median cracks form at the elastic-plastic boundary, also from pre-existing flaws or by plasticity, and form sub-surface penny-like cracks immediately below the indenter. These cracks grow on further loading and may engulf the radial nuclei before the unloading cycle is begun. Alternatively, the median cracks may form at a load not greatly in excess of that required to form the radial cracks. On unloading then, both crack systems grow simultaneously with the radial system confined to the near-surface region. As unloading nears completion, the median cracks may merge with, or engulf, the radial cracks [15] resulting in a final crack pattern identical to the one outlined above.

A third situation may arise in which the load is insufficient to form a penny-like median crack but in excess of that necessary to initiate the radial system (Fig. 6a). In this situation the surface radial cracks may grow on unloading, merging beneath the indenter tip to once again obtain the classic Vickers crack pattern (Fig. 6b).

The Chiang, Marshall and Evans model of crack initiation about an indenter explains many of the features observed in indentation crack patterns and is the most recent advanced.

3.2. Propagation

The distribution of the 'far-field' stresses which influence the growth of an initiated crack are less controversial than that of the 'near-field'.

Once removed from the vicinity of the contact site, the stresses in the material are elastic.

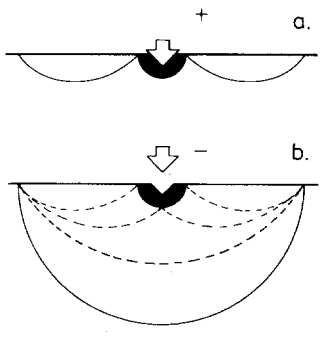

Fig. 6. Half-penny radial crack formation resulting solely from surface radial (Palmqvist) cracks. Loading (+) and unloading (−) cycles are as indicated.

The equations for the components of these elastic stresses about a point indentation in an isotropic material were first formulated by Boussinesq in 1885 [47]. From these equations stress contours of the three principal normal stresses (Fig. 7) may be determined. The σ_{11} and σ_{33} stresses (see insert, Fig. 7) both lie in planes of symmetry through the load axis with σ_{11} everywhere tensile and σ_{33} everywhere compressive. The σ_{22} 'hoop' stress is tensile to within approximately 52 deg of the surface and compressive elsewhere.

The Boussinesq equations showed the stress field to be partially dependent on the Poisson's ratio (ν) of the material involved. Lawn and Swain [22] claimed the Poisson's ratio greatly affected the maximum tensile stress which was found to disappear altogether for $\nu = 0.5$. Since cracks tend to propagate nearly-orthogonal to major tensile stresses [48] and since the indentation technique is best suited to essentially brittle fracture, the Poisson's ratio of the indented material must be chosen so that a maximum tensile stress exists and the material is brittle.

Materials generally range from highly brittle to highly ductile for Poisson's ratio between 0.2 to 0.5 [49]. Hence, in order to obtain a stress field which will result in a well defined crack (i.e. a crack which is large in comparison to the indent and so is governed by the far-field stresses), the indented material should have a Poisson's ratio to the lower end of this range.

Once initiated, a crack originating immediately below the indenter tip in a material of small Poisson's ratio will propagate downwards into the material (in the σ_{33} direction) maintaining orthogonality with the σ_{11} and σ_{22} tensile stresses (Fig. 7). The crack will also expand outwards in the σ_{11} direction in order to remain orthogonal to the σ_{22} tensile stress, ultimately resulting

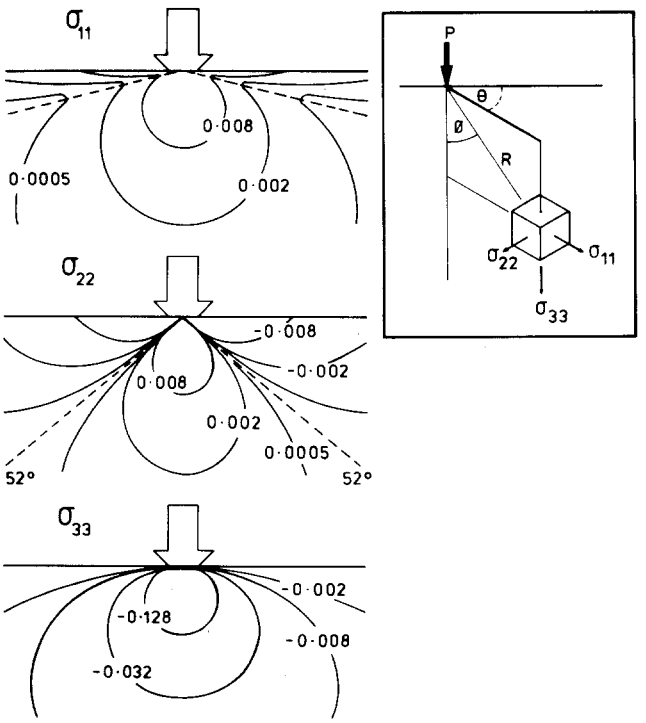

Fig. 7. Contours of the three principal normal stresses (see insert) associated with a Boussinesq stress field (after Lawn and Swain, [22]). These stresses have the general form

$$\sigma_{ij} = \left(\frac{P}{\pi R^2}\right) \cdot f_{ij}(\phi) \cdot \nu$$

where P, R and ϕ are as defined in the insert and ν = Poisson's ratio for an isotropic material.

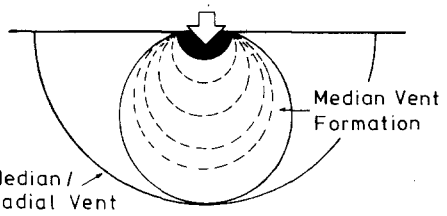

Fig. 8. Enclosed 'full-penny' median vent formation beneath a sharp indenter as loading progresses. Radial vent formation (usually) occurs upon indenter removal but may also be induced during loading.

in the enclosed full-penny configuration (Fig. 8). This sideways expansion will, however, be limited by the compressive lobes of the hoop stress at angles of less than approximately 52 deg to the surface.

Upon unloading, the material attempts to regain its stored elastic energy. The plastic zone, being the most highly deformed region, undergoes the most severe contraction but is inhibited by the surrounding material. The residual tensile stress thus formed in the material surrounding the contact site drives the full-penny median vent to the equilibrium half-penny median-radial configuration maintaining near-orthogonality to the σ_{11} radial tensile stress.

Alternatively, loading continues until the enclosed penny-like crack is able to break through the confining compressive stress lobes to once again form the median-radial configuration.

4.0. Real indenters

The stress field situations outlined above for crack initiation and propagation about a sharp indenter apply to an idealized case. This idealized approach has evolved as a matter of necessity since real indenter/material interactions are extremely complex in nature requiring some simplifications before an analysis is attempted. Of special interest in relation to indentation toughness testing are the effects of anisotropy, particle size, environment and residual stresses.

4.1. Anisotropy

The symmetrical stress fields shown in Fig. 7 apply to those found in an isotropic material. Consequently, the crack pattern resulting from a Vickers indentation in annealed soda-lime glass shows symmetrical surface traces of equal length emanating from all four corners of an equi-axed hardness impression.

An asymmetric crack pattern might then be expected to result from an indentation in an anisotropic material. This has been observed by workers in relation to orientation effects in ionic solids [28,50].

Similarly, an indentation in a material with an anisotropic grain structure might be expected to produce an asymmetric crack pattern.

4.2. Particle size effects

Coarse grained polycrystalline materials (i.e. grain size comparable to plastic impression size) may produce a crack pattern not truly indicative of the material as a whole. As the grain size increases anisotropy within the grains becomes more prevalent until, in the extreme where grain size > indent size, a pattern indicative of the individual grains results.

Attempting to overcome this problem by increasing the load, however, produces a greater

tendency to chipping (i.e. lateral vents intersecting the surface) and subsequent obscurity of the crack pattern [11].

Evans [36] claimed the crack patterns to be more prone to disruption by individual grains as the grain size is increased, while material inhomogeneities of > 1 μm are considered by some authors to affect the crack pattern [51].

It has also been suggested that the nucleation and propagation of the various crack systems is influenced by grain size effects [39].

4.3. Environmental effects

Sharp contact events have associated with them a residual stress field. Cracks in the material (either pre-existing or induced by the contact) may then undergo slow crack growth in the presence of a suitable environment under the influence of this residual stress. Post-indentation crack growth has been observed in a number of indentation studies [1,40,52–55] and can lend to an under-estimation of material toughness.

4.4. Residual stresses

It is likely that the Boussinesq stress field (and hence, indentation toughness value) may be significantly altered by the superposition of pre-existing residual stresses in the material.

This has been dramatically evidenced in the case of soda-lime glass where the introduction of compressive residual surface stresses resulted in suppression of radial crack formation [34].

Other workers have also noted the influence of pre-existing stresses [56] resulting from surface grinding and tempering on the behaviour of materials subjected to sharp contact events [57–59].

5.0. Toughness determination using the median radial crack system

The first quantitative use of the median-radial crack system for evaluating material fracture toughness was that of Palmqvist in his empirical study of metal carbides [29]. The development of this method of toughness testing from Palmqvist to more current times has recently been reviewed [60] and so will not be presented here. Instead, a derivation of the current equation based on the original approach of Lawn and Fuller [10], will be given. Although simplistic, this approach highlights many of the important aspects of indentation fracture toughness testing.

The direct observation of median-radial crack formation in glass during a sharp contact event revealed that:

(1) Well developed indentation cracks have near-circular crack fronts at advanced stages of loading (this is also true of blunt indenters) and,
(2) The impressions left by an indenter at various loads are geometrically similar, i.e. the indentation pressure is load independent [10].

These two observations may be used to derive an equation relating material fracture toughness (K) to the indentation parameters of load (P), crack length (C) and indentation impression size (a) as defined in Fig. 9.

The observation of penny-like cracks at advanced loading allows the application of the Griffith energy-balance criterion [61], in conjunction with a scalar argument, to determine the energy-balance requirements for such cracks at equilibrium. This approach is much the same as that used by Roesler [3] in his analysis of blunt indenters.

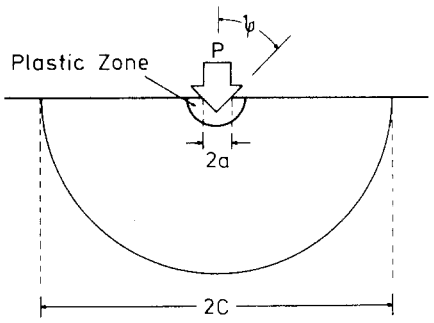

Fig. 9. Schematic representation of a sharp contact event showing the indentation parameters of load (P), indenter half-angle (ψ), impression diagonal (a) and surface crack length (C) required for the determination of material fracture toughness.

The Griffith equation may be expressed as

$$\frac{dU_e}{dC} = -\frac{dU_\gamma}{dC} \tag{1}$$

where U_e = the elastic energy stored in the body and U_γ = the surface free energy of the crack

For a circular crack of fracture surface energy (γ), the total surface energy must scale as

$$U_\gamma \alpha \gamma \cdot C^2.$$

The evaluation of the U_e term relies on the observation of geometrical similarity. For well developed cracks the far-field stresses control behaviour. Geometrical similarity ensures that these stress fields are load independent and similarly distributed and can therefore be expressed by a Boussinesq stress distribution (σ_{ij}). The stress (σ) over a crack of length C must then scale as

$$\sigma = \sigma_{ij} \alpha \frac{P}{\pi \cdot C^2}. \tag{2}$$

The strain energy density (strain energy/unit volume, V) of a material is defined as

$$\frac{U_e}{V} = \frac{\sigma^2}{2 \cdot E}$$

where E = Young's modulus.

By substitution of (2) then, the strain energy density of a material under the influence of a Boussinesq field is found to vary as

$$\frac{U_e}{V} \alpha \frac{P^2}{2 \cdot C^4 \cdot E}.$$

The total strain energy in the volume of material influenced by the crack ($V \alpha C^3$) is then found to be

$$U_e \alpha \frac{P^2}{C \cdot E}.$$

Invoking (1) after substitution of the U_γ and U_e terms produces

$$A \cdot \gamma \cdot \frac{d}{dC}(C^2) = \frac{B \cdot P^2}{E} \cdot \frac{d}{dC}\left(\frac{1}{C}\right)$$

where A, B = proportionality constants.

This then gives the equilibrium condition for penny-like cracks in a Boussinesq field (in a

given material) as

$$\frac{P^2}{C^3} = M$$

or

$$\frac{P}{C^{3/2}} = N \tag{3}$$

where M, N = constants.

Equation (3) is of the same form as the stress intensity factor (K) for a plane circular crack of radius C in a solid subjected to a uniform stress (σ) acting perpendicular to the crack plane [62] i.e.

$$K = 2 \cdot \sigma \cdot \sqrt{\frac{C}{\pi}} = 2 \cdot \frac{P}{\pi \cdot C^2} \sqrt{\frac{C}{\pi}}$$

giving

$$K = \frac{2}{\pi^{3/2}} \cdot \frac{P}{C^{3/2}} \text{ or } \frac{P}{C^{3/2}} = \text{constant (since } K \text{ is constant for a given material).}$$

It was therefore concluded that the fracture toughness (K_c) of a material which exhibits geometrical similarity and a circular crack front at advanced loading may be determined from sharp indentation crack patterns according to

$$K_c = \chi \cdot \frac{P}{C^{3/2}} \tag{4}$$

where χ = constant and P = load required to produce a crack of characteristic dimension C (Fig. 9).

A more analytical approach adopted by Lawn, Evans and Marshall [16] later showed that this equation contained contributions from both the reversible elastic (K_e), and the irreversible residual (K_r), stress field components of the indentation field. Both these components have the same form as (4). They also established the value of the constant for radial crack formation to be

$$\chi_r = \xi \cdot (\cot \psi)^{2/3} \cdot \left(\frac{E}{H}\right)^{1/2}$$

where ψ = indenter half-angle, H = material hardness = $P/(2.a^2)$, ξ = experimentally determined constant independent of indenter/specimen system, $= 0.032 \pm 0.002$.

Substitution of this into (4) (taking $\psi = 68$ deg for a Vicker's indenter) then gives

$$K_c = 0.02473 \cdot E^{1/2} \cdot a \cdot \frac{P^{1/2}}{C^{3/2}}. \tag{5}$$

Vickers, rather than Knoop, indentations are preferred for toughness measurements in most cases for a variety of reasons [63,64].

The median/radial crack system is most commonly used to determine fracture toughness since it produces a surface trace, an advantage in opaque materials, and attains equilibrium only after indenter removal. The elastic stress field component contribution to the fracture toughness can therefore be ignored.

From the above derivation and Section 4, (5) may be considered as applicable only if the following conditions are met:

(1) The material being tested should be of sufficient thickness to ensure the extent of the far-field stresses is such as to allow the development of the median-radial crack system without modification of these stresses as a result of edges. A material thickness exceeding 10 times the indentation crack length has been suggested as suitable [51].

(2) The crack must be circular at advanced loading (or semi-circular at complete unload) i.e.

$$\frac{P}{C^{3/2}} = \text{constant}.$$

(3) The material must be initially stress free so that the stresses on the crack during loading are attributable solely to the Boussinesq stress field produced by the indentation.
(4) $C > 2a$ (see Fig. 9) without chipping. This ensures a clearly visible, well developed crack influenced only by the far-field (Boussinesq) stresses. Lateral vent formation, which can lead to chipping, is known to reduce the intensity of the residual stress field [65].
(5) The test material must be reasonably homogeneous over the scale of the impression to avoid variations in crack length and,
(6) In polycrystalline materials the grain size must be small in comparison to the indentation size to avoid possible disruption of the crack pattern.

6.0. Conclusion

By recognizing the limitations associated with indentation toughness testing this method has been successfully employed to determine the toughness of certain polycrystalline materials to within 10 percent [66]. However, recent work on densification effects [67] and superposition of external stress fields over the indentation residual stress field [59], suggests that indentation fracture theory is progressing to the stage where many of these current limitations may soon be incorporated into existing theory. This should then increase the range of application of indentation fracture toughness testing and so provide a versatile tool for materials examination.

Acknowledgements

The authors would like to express their thanks to Dr M.V. Swain for his contribution, in the form of useful discussions, to this work. The similar contributions of Dr P.F. Thomson and Dr. J.R. Griffiths are also gratefully acknowledged.

References

1. B.R. Lawn and T.R. Wilshaw, *Journal of Materials Science* 10 (1975) 1049–1081.
2. H.R. Hertz in *Hertz's Miscellaneous Papers,* MacMillan Press, London (1882) Chapters 5, 6.
3. F.C. Roesler, *Proceedings of the Royal Society,* Series B. 69 (1956) 981–992.
4. F.C. Frank and B.R. Lawn, *Proceedings of the Royal Society,* Series A 299 (1967) 291–306.
5. B.R. Lawn, *Journal of Applied Physics* 39 (1968) 4828–4836.
6. A.G. Mikosza and B.R. Lawn, *Journal of Applied Physics* 42 (1971) 5540–5545.
7. B.R. Lawn, T.R. Wilshaw, and N.E.W. Hartley *International Journal of Fracture* 10 (1974) 1–16.
8. K.L. Johnson, J.J. O'Connor, and A.C. Woodward, *Proceedings of the Royal Society,* Series A 334 (1975) 95–117.
9. B.J. Hockey and B.R. Lawn, *Journal of Materials Science* 10 (1975) 1275–1284.
10. B.R. Lawn and F.R. Fuller, *Journal of Materials Science* 10 (1975) 2016–2024.
11. B.R. Lawn, M.V. Swain and K. Phillips, *Journal of Materials Science* (Letters) 10 (1975) 1236–1239.
12. S.M. Wiederhorn and B.R. Lawn, *Journal of the American Ceramic Society* 60 (1977) 451–458.
13. M.M. Chaudhri and P.A. Brophy, *Journal of Materials Science* 15 (1980) 345–352.
14. B.R. Lawn, F.R. Fuller and S.M. Wiederhorn, *Journal of the American Ceramic Society* 59 (1976) 193–197.
15. A.G. Evans and T.R. Wilshaw, *Acta Metallurgica* 24 (1976) 939–956.
16. B.R. Lawn, A.G. Evans and D.B. Marshall, *Journal of the American Ceramic Society* 63 (1980) 574–581.
17. B.R. Lawn and D.B. Marshall, in *Fracture Mechanics of Ceramics,* 3, Plenum Press, N.Y. (1978) 205–229.
18. B.R. Lawn and A.G. Evans, *Journal of Materials Science* 12 (1977) 2195–2199.
19. R. Hill, *The Mathematical Theory of Plasticity*, Clarendon Press, Oxford (1950) 97–106.
20. D.M. Marsh, *Proceedings of the Royal Society*, Series A 279 (1964) 420–435.
21. K.L. Johnson, *Journal of the Mechanics and Physics of Solids* 18 (1970) 115–126.
22. B.R. Lawn and M.V. Swain, *Journal of Materials Science* 10 (1975) 113–122.
23. J.T. Hagan and S. Van der Zwaag, *Journal of Non-Crystalline Solids* 64 (1984) 249–268.

24. J.T. Hagan, *Journal of Materials Science* 15 (1980) 1417–1424.
25. J.T. Hagan, *Journal of Materials Science* 14 (1979) 462–466.
26. W. Hirst and M.G.J.W. Howse, *Proceedings of the Royal Society,* Series A 311 (1969) 429–444.
27. C.M. Perrot, *Wear* 45 (1977) 293–309.
28. J.T. Hagan, *Journal of Materials Science* 14 (1979) 2975–2980.
29. S. Palmqvist, *Jernkontorets Ann* 141 (1957) 300–307.
30. I.M. Ogilvy, C.M. Perrot and J.W. Suiter, *Wear* 43 (1977) 239–253.
31. J.T. Hagan and M.V. Swain, *Journal of Physics,* Series D 11 (1978) 2091–2102.
32. J. Lankford and D.L. Davidson, *Journal of Materials Science* 14 (1979) 1669–1675.
33. J. Lankford, *Journal of Materials Science* 16 (1981) 1177–1182.
34. T. Haranoh, H. Ishikawa, N. Shinkai and M. Mizuhashi, *Journal of Materials Science* 17 (1982) 1493–1500.
35. S.S. Chiang, D.B. Marshall and A.G. Evans, *Journal of Applied Physics* 53 (1982) 298–311.
36. A.G. Evans, STP 678, *Fracture Mechanics Applied to Brittle Materials*, ASTM, Philadelphia (1979) 112–135.
37. D.B. Marshall, B.R. Lawn and P. Chantikul, *Journal of Materials Science* 14 (1979) 2225–2235.
38. S.S. Chiang, D.B. Marshall and A.G. Evans, *Journal of Applied Physics* 53 (1982) 312–317.
39. S. Van der Zwaag, J.T. Hagan and J.E. Field, *Journal of Materials Science* 15 (1980) 2965–2975.
40. B.R. Lawn, T.P. Dabbs and C.J. Fairbanks, *Journal of Materials Science* 18 (1983) 2785–2797.
41. K.W. Peter, *Journal of Non-Crystalline Solids* 5 (1970) 103–115.
42. B.J. Hockey, *Journal of the American Ceramic Society* 54 (1971) 223–231.
43. M.V. Swain, *Journal of the American Ceramic Society* (Discussion and Notes) 62 (1979) 318–319.
44. B.R. Lawn and D.B. Marshall, *Journal of the American Ceramic Society* (Discussion and Notes) 62 (1979) 106–108.
45. J. Lankford, *Journal of Materials Science* (Letters) 1 (1983) 493–495.
46. D.K. Shetty and I.G. Wright, *Journal of Materials Science* (Letters) 5 (1986) 365–368.
47. J. Boussinesq, (1885) Discussed in *Theory of Elasticity*, McGraw-Hill, N.Y. (1970) 398–402.
48. B.R. Lawn and T.R. Wilshaw, *Fracture of Brittle Solids*, Cambridge University Press, Cambridge (1975).
49. A. Kelly, *Strong Solids*, Clarendon Press, Oxford (1966).
50. J. Lankford and D.L. Davidson, *Journal of Materials Science* 14 (1979) 1662–1668.
51. G.R. Anstis, P. Chantikul, B.R. Lawn and D.B. Marshall, *Journal of the American Ceramic Society* 64 (1981) 533–538.
52. M.V. Swain, J.S. Williams, B.R. Lawn and I.J.H. Beek, *Journal of Materials Science* 8 (1973) 1153–1164.
53. M.G. Mendiratta and J.J. Petrovic, *Journal of the American Ceramic Society* 61 (1978) 226–230.
54. P.K. Gupta and N.J. Jubb, *Journal of the American Ceramic Society* 64 (1981) C 112– C 114.
55. P. Ostojic and R. McPherson, in *Proceedings of the 10th Australian Ceramics Conference,* August 24–27, Melbourne, Australia (1982) 189–193.
56. P. Chantikul, B.R. Lawn and D.B. Marshall, *Journal of the American Ceramic Society* 62 (1979) 340–343.
57. D.B. Marshall and B.R. Lawn, *Journal of Materials Science* 14 (1979) 2001–2012.
58. R.F. Cook, B.R. Lawn, T.P. Dabbs and P. Chantikul, *Journal of the American Ceramic Society* 64 (1981) C 121–122.
59. D.B. Marshall, A.G. Evans, B.T. Khuri Yakub, J.W. Tien and G.S. King, *Proceedings of the Royal Society,* Series A 385 (1983) 461–475.
60. J.G.P. Binner and R. Stevens, *Transactions and Journal of the British Ceramic Society* 83 (1984) 168–172.
61. A.A. Griffith, *Proceedings of the Royal Society, Philosophical Transactions*, Series A 221 (1921) 163–198.
62. D.P. Rooke and D.J. Cartwright, in *Compendium of Stress Intensity Factors* Hillingdon Press, Middlesex, England (1976) 270.
63. D.B. Marshall, *Journal of the American Ceramic Society* 66 (1983) 127–131.
64. J.J. Petrovic, *Journal of the American Ceramic Society* 66 (1983) 277–283.
65. B.R. Lawn, D.B. Marshall, and P. Chantikul, *Journal of Materials Science* 16 (1981) 1769–1775.
66. M.J. Majdic and G. Ziegler, *Zeitung für Werkstofftechnologie* 13 (1982) 226.
67. R.F. Cook and B.R. Lawn, *Journal of the American Ceramic Society* 66 (1983) C 200–C 201.

Résumé. On souligne l'influence de l'émoussage ou de l'acuité d'un poinçon lors de la production de fissures d'indentation. On se concentre ensuite sur l'amorçage et la propagation de fissure résultant du contact avec un poinçon à angle acéré, cas le plus intéressant dans la pratique, et d'usage courant pour déterminer la ténacité à la rupture de matériaux vitreux. On discute brièvement de l'influence que l'anisotropie, la taille des particules, l'environnement et les contraintes résiduelles peuvent avoir sur le comportement de telles fissures. On donne également une dérivée simpliste de la formule couramment utilisée pour la détermination de la ténacité à la rupture des matériaux adéquats à partir d'une essai de poinçonnage. On présente également les critères pour que les résultats soient valides, et on indique comment ces critères, en association avec d'autres points évoqués par ailleurs, mettent en lumière les limites de cette méthode.